國立交通大學

光電工程研究所

碩 士 論 文

低臨界值半導體雷射激發摻釹釩酸釔被動鎖模雷射在半導體飽和吸收鏡及非線性鏡之相關研究

Low Threshold Passively Mode-Locked Diode-Pumped Nd:$GdVO_4$ Laser by Semiconductor Saturable Absorber and Nonlinear Mirror

研 究 生：楊文勛

指導教授：謝文峰　教授

中 華 民 國 九 十 四 年 六 月

國立交通大學

光電工程研究所

碩 士 論 文

低臨界值半導體雷射激發摻釹釩酸釔被動鎖模雷射在半導體飽和吸收鏡及非線性鏡之相關研究

Low Threshold Passively Mode-Locked Diode-Pumped Nd:$GdVO_4$ Laser by Semiconductor Saturable Absorber and Nonlinear Mirror

研 究 生：楊文勛

指導教授：謝文峰　教授

中 華 民 國 九 十 四 年 六 月

Low Threshold Passively Mode-Locked Diode-Pumped Nd:$GdVO_4$ Laser by Semiconductor Saturable Absorber and Nonlinear Mirror

Student: Wen-Hsun Yang

Advisor: Dr. Wen-Feng Hsieh

A Thesis

Aubmitted to Institute of Electro-Optical Engineering

College of Electrical Engineering and

Computer Science

National Chiao Tung University

In Partial Fulfillment of the Requirements

for the Degree of

Master

In

Electro-optical Engineering

June 2005

Hsin-chu，Taiwan，Republic of China

Low Threshold Passively Mode-Locked Diode-Pumped Nd:$GdVO_4$ Laser by Semiconductor Saturable Absorber and Nonlinear mirror

Student: Wen-Hsun Yang Advisor: Prof. Wen-Feng Hsieh

Institute of Electro-optical Engineering

National Chaio Tung University

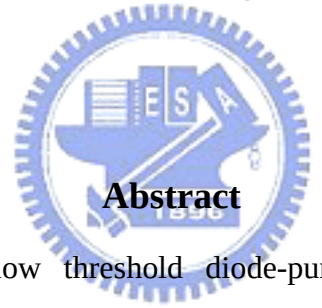

Abstract

We demonstrated low threshold diode-pumped passively mode-locked Nd:$GdVO_4$ laser by using semiconductor satiable absorber mirror (SESAM) and nonlinear mirror (NLM). The measured thresholds of continuous wave mode-locking (CML) agree well with the theoretically calculated values considering the critical intracavity power for stability of CML against the Q-switching mode-locking (QML). Besides, we have for the first time observed the harmonic mode locking and pulse splitting by varying the distance between KTP and dichroic mirror in the NLM picosecond laser.

低臨界值半導體雷射激發摻釹釩酸釔被動鎖模雷射在半導體飽和吸收鏡及非線性鏡之相關研究

研究生: 楊文勛　　指導教授: 謝文峰 教授

國立交通大學光電工程研究所

摘要

我們分別利用半導體飽和吸收鏡以及非線性鏡鎖模兩種方式，得到了低臨界值連續波鎖模的摻釹釩酸釔皮秒脈衝雷射輸出。在實驗中，我們所得到的連續波鎖模臨界值，與考慮連續波鎖模穩定條件之理論計算出的數值非常吻合。除此之外，我們也首次在非線性鏡鎖模皮秒雷射中觀察到，伴隨著改變 KTP 晶體以及雙色鏡之間的距離時，會出現諧頻鎖模以及脈衝分裂的現象。

Acknowledgements

一轉眼，兩年的碩士生涯就將要結束了，而我也逐漸在老師和學長的指導下，一點一滴的進步和成長。在此，我要感謝謝文峰老師，多虧老師耐心的指導及糾正，我才能跟上大家的腳步，並且逐漸掌握一個研究生該有的能力。當然，我也要感謝家弘學長，從實驗的起頭到實驗的終了，不論是處理數據亦或是實驗技巧，學長都不斷的在給我助力，讓我學到很多。而整個實驗室的愉快氣氛也不斷的在影響著我：小戴學長在我緊張時給我的鼓勵、智章學長在我有疑問時給我的解答、阿政學長風趣、維仁學長對美女的見解、松哥的增胖計劃、學姊(晴如姊)和學弟間的美女式流氓對話、阿笑與蟑螂的對決、小豪不斷進步的歌聲、阿峰適時的救援、小毅的流利水果刀法、阿斌與電動戰爭、鄭信民學長的保齡球神功、大師兄養車的經驗、奎哥的怪物級體力以及逢賭必輸的學弟榕哥，還有已經畢業的學長姊以及剛進實驗室的碩零學弟妹。在實驗室的兩年，從研究進入生活，從生活融入研究，這已經是我無法忘卻的珍貴回憶了 (我沒有忘記臭臭的實驗室助理兼貪吃鬼-奶油)。

最後，我親愛的家人們，在這兩年間給我的支持，不論是精神或是物質，都是無可取代的，謝謝你們。

感謝國科會計畫編號 NSC93-2112-M-009-035 的經費支持，使得研究得以順利完成。

感謝的話說不完，但是我還是要說，謝謝大家在這兩年間對我的照顧。

List of figures

Content

Chapter 1 Introduction

1.1. Introduction

The compact all-solid diode pumped infrared picosecond Nd^{3+} doped lasers have attracted much attention for various applications such as optical communication, nonlinear optical spectroscopy, optical frequency conversion, microsurgery and biomedicine. Recently, other than Nd:YVO_4, the Nd:$GdVO_4$ laser crystal has become great interest due to its good physical, optical, and mechanical properties. The relatively broader gain bandwidth and unexpectedly higher thermal conductivity of the Nd:$GdVO_4$ than the Nd:YVO_4 makes it favorable for mode-locking with much narrower pulse duration that provides the desirable high-peak power [1]. Recently, intra-cavity saturable abosorber [2, 3] and semiconductor saturable absorber mirror (SESAM) [4, 5] have been used for passively mode-locking Nd:$GdVO_4$ laser.

For generating femtosecond pulse trains [6] natural fast saturable absorber utilizing the inherent self-focusing nonlinearity of the laser crystal has been widely used to self mode-lock the solid state lasers. However, it is more problematic for picosecond lasers due to their low peak intensity in turn having weak nonlinear modulation. Fortunately, the nonlinear mirror (NLM) mode locking provides strong nonlinear loss modulation that was first time proposed by Stankov [7]. The NLM consists of a nonlinear crystal placed in front of an output coupler in the laser cavity. The output coupler provides 100% reflection at the second harmonic wave (SH) and partial reflection at the fundamental wave (FW). If the SH experiences an appropriate phase shift with respect to the FW before the second pass through the nonlinear crystal, then the reflected SH may be completely converted back to the FW. It had been demonstrated in Nd:YAG

lasers [8-9] and Nd:YVO4 [10-13] lasers in use of various nonlinear crystals including KTP, PPKTP and LBO, but it has not been investigated carefully in Nd:$GdVO_4$ to our knowledge.

1.2. Motivation

High power picosecond mode-locked lasers with stable laser output and low threshold against Q-switching mode-locking (QML) are required for many applications, in particular for those involving microsurgery and biomedicine. However, until recently the stable CW mode-locking (CML) are generated at high pumping power [5,11].

In this thesis, we use Nd:$GdVO_4$, SESAM and NLM to set up the low threshold picosecond passive mode-locking laser. There is still no complete investigation about passive mode-locking Nd:$GdVO_4$ laser in using nonlinear mirror, to our knowledge.

1.3. Organization of the thesis

This thesis consists of five chapters, including present introduction and motivation. Chapter 2 reviews the basic principles of mode-locking lasers. In chapter 3 and chapter 4, we show the measurement and experimental results of the passively mode-locking Nd:$GdVO_4$ laser with SESAM and NLM. In the final chapter, we conclude the researching work from the experimental analysis and give the blueprinted plan in future work.

Chapter 2 Basic Principles and Mechanisms of Mode Locking

2.1. Mode locking

Mode locking is the most important method of generating ultrashort light pulses [14]. Basically, it's attained by locking together all of the phases belonging to different longitudinal modes of a laser. Locking of these modes is achieved by periodically modulating the loss (or gain) inside the resonator. In this section we will describe the basic principles of mode locking, especially, the mechanism of passive mode-locking.

Consider a laser contains a gain medium either homogeneously or inhomogenerously broadened with a bandwidth which can support numbers of longitudinal modes separated by

$$\omega_q - \omega_{q-1} = \frac{\pi c}{l} \equiv \Omega, \tag{2-1}$$

where l is the cavity length and ω is the longitudinal frequency, the total optical electric field resulting from such multimode oscillation can be expressed as

$$e(t) = \sum_n E_n e^{i[(\omega_0 + n\Omega)t + \phi_n]} + c.c., \tag{2-2}$$

where the summation is extended over total numbers N of the oscillation modes and ω_0 is chosen as the central frequency of these modes, ϕ_n is the phase of the nth mode and c.c. stands for complex conjugate. One property of (2-2) is that e(t) is periodic in $T \equiv 2\pi/\Omega \equiv 2l/c$ if ϕ_n are independent of time and T is the round-trip transit time inside the resonator, one obtains

$$e(t+T)=\sum_n E_n e^{\{i[(\omega_0+n\Omega)(t+\frac{2\pi}{\Omega})+\phi_n]\}}$$
$$=\sum_n E_n e^{\{i[(\omega_0+n\Omega)t+\phi_n]\}} e^{\{i[2\pi(\frac{\omega_0}{\Omega}+n)]\}} . \qquad (2\text{-}3)$$
$$=e(t)$$

sine ω_0/Ω is an integer ($\omega_0=m\pi c/l$) and $\exp[2\pi i(\omega_0/\Omega+n)]=1$. Generally, the phases ϕ_n are likely to vary randomly with time. This causes the intensity of the laser to fluctuate randomly and greatly reduce its usefulness for many applications for which temporal coherent is important [15].

Two ways in which the laser can be made coherent: The first approach is to make it possible for the laser to oscillate at a single frequency only so that mode interference is eliminated. This can be achieved in a variety of ways, including shortening the resonator length l, thus increasing the mode spacing ($\omega_0=\pi c/l$) to allow only one mode having sufficient gain to oscillate. The second approach is to force the phases ϕ_n of all the longitudinal modes to maintain their relative values. This is the so-called mode locking technique proposed and demonstrated in the early history of the laser [16]. This mode locking technique forces the laser intensity to change as a periodic train with a period of $T=2l/c=2\pi/\Omega$.

One of the most useful form of mode locking results if the phases ϕ_n are made all equal. To simplify the analysis of this case, we assume that these N oscillating modes have the same amplitudes and phases, $E_n=1$ and $\phi_n=0$, and (2-1) gives

$$e(t)=\sum_{-(N-1)/2}^{(N-1)/2} e^{i(\omega_0+n\Omega)t}$$
$$=e^{i\omega_0 t}\frac{\sin(\frac{N\Omega t}{2})}{\sin(\frac{\Omega t}{2})}. \qquad (2\text{-}4)$$

The average laser output power is proportional to e(t)e*(t) and is given by

$$P(t) \propto \frac{\sin^2(\frac{N\Omega t}{2})}{\sin^2(\frac{\Omega t}{2})}. \qquad (2\text{-}5)$$

And some of the analytic properties of P(t) are immediately apparent:

1. The power is emitted in a form of a train of pulse with a period T=2*l*/c=2π/Ω, which is equal to the round-trip time.
2. The peak power, P(sT)(for s=1, 2, 3,…), is equal to N times the average power, where N is the number of modes locking to one another.
3. The peak field amplitude is equal to N times the amplitude of a single mode.
4. The individual pulse width, defined as the time from the peak to the first zero is τ_0=T/N. The number of oscillation modes can be estimated by N≈$\Delta\omega$/Ω that is, the ratio of the transition line width $\Delta\omega$ to the longitudinal frequency spacing Ω between modes.
5. Using this relation, as well as T=2π/Ω in τ_0=T/N, we obtain

$$\tau_0 \sim \frac{2\pi}{\Delta\omega} = \frac{1}{\Delta\upsilon}. \qquad (2\text{-}6)$$

Thus the width of the mode-locked pulses is approximately the inverse of the gain bandwidth.

2.2. Passive Mode locking with SESAM

In this section we review the theory developed by Kaörtner et al. [17] which has been confirmed to be very accurate for picosecond lasers, and introduce the notation used below. In the cw mode-locking (CML) regime [Fig. 2.1] the laser generates a train of mode-locked pulses with high amplitude stability, while Q-switching mode-locking (QML) [Fig. 2.1] means that the amplitude of mode-locked pulses is modulated with a strongly peaked Q-switching envelope.

To derive a stability criterion of CML against QML, they start from the rate equations for the intracavity power, gain, and saturable absorption. The rate equations for the mode-locked laser can be written as

$$\frac{dP}{dt} = \frac{g - l - q_p(E_p)}{T_R} P, \qquad (2\text{-}7)$$

$$\frac{dg}{dt} = -\frac{g - g_0}{\tau_L} - \frac{P}{E_{sat,L}} g, \qquad (2\text{-}8)$$

$$\frac{dq}{dt} = -\frac{q - q_0}{\tau_A} - \frac{P}{E_{sat,A}} q, \qquad (2\text{-}9)$$

where P is the average intracavity laser power, T_R is the cavity round-trip time, $E_p = PT_R$ is the intracavity pulse energy, g is the time-dependent round-trip power gain coefficient, q is the time-dependent round-trip power saturable absorption coefficient, g_o and q_o are the corresponding quantities in equilibrium with no intracavity power, τ_L is the upper-state lifetime of the laser medium, τ_A is the upper-state lifetime of the absorber recovery time, $E_{sat,L}$ is the saturation energy of the gain, and $E_{sat,A}$ is the saturation energy of the absorber, respectively. $q_p(E_p)$ in Eq. 2-7 represents the round-trip loss introduced by the saturable absorber for a given intracavity pulse energy. We make two assumptions to determine q_p. First, we assume SESAM is a slow absorber. Second, the absorber recovery time τ_A must be much shorter than the cavity round-trip time T_R. Then for the pulse energy loss per round trip, we obtain

$$q_p(E_p) = q_o \frac{F_{sat,A} A_{eff,A}}{E_p} [1 - \exp(-\frac{E_p}{F_{sat,A} A_{eff,A}})]. \qquad (2\text{-}10)$$

Using this result, we can describe the mode-locked laser by (2-7) and (2-8). After linearizing these equations for small deviations δE_p and δg from the steady-state value, $\overline{E_p}$ and $\overline{g}$ in analogy to the analysis given in Ref. 18, we

obtain the criterion

$$E_p \left| \frac{dq_p}{dE_p} \right|_{\overline{E_p}} < \frac{T_R}{\tau_L} r = \frac{T_R}{\tau_L} + \frac{E_p}{E_{sat,L}}$$
$$r = 1 + P / P_{sat,L}, \qquad (2\text{-}11)$$

for stability of CML against QML. Since we used semiconductor saturable absorber mirror (SESAM) as the passive mode locker, whose nonlinear reflectivity is

$$R(E_p) = R_{ns} \frac{\ln\{1 + \exp(-\Delta R)[\exp(\frac{E_p}{E_{sat,A}}) - 1]\}}{E_p / E_{sat,A}}, \qquad (2\text{-}12)$$

derived from a simple model for nonlinear pulse propagation in the absorber. Here ΔR is the maximum change in nonlinear reflectivity and R_{ns} is the reflectivity for high pulse energy. For absorbers with ΔR smaller than approximately 10%, we can simplify (2-12) to

$$R(E_p) = R_{ns}\{1 - \Delta R \frac{F_{sat,A} A_{eff,A}}{E_p}\} \times [1 - \exp(-\frac{E_p}{E_{sat,A} A_{eff,A}})]. \qquad (2\text{-}13)$$

The nonlinear reflectivity of the SESAM is related to the pulse energy loss per round trip.

We did not include any nonsaturable losses in q(t) [(2-9)] or $q_p(E_p)$ [(2-10)]. For passively mode-locked solid-state lasers we can assume that the modulation depth is small, i.e., $\Delta R \ll 1$. Therefore the maximum modulation depth is given by $\Delta R = 1 - \exp(-q_o) \approx q_o$ for $\Delta R \ll 1$. In addition, the nonsaturable losses should be as low as possible because they only degrade the laser performance. For stable mode locking we typically have to use a small transmission output coupler (T_{out}) of the order of a few percent, which results in the additional condition that $\Delta R \ll T_{out} \ll 1$. Therefore we can make the approximation that $R_{ns}=1$ and

$$R(E_p) \approx \exp[-q_p(E_p)] \approx 1 - q_p(E_p). \qquad (2\text{-}14)$$

Then the approximation of the stability criterion of CML against QML with the nonlinear reflectivity can be rewritten as

$$E_p \left. \frac{dR(E_p)}{dE_p} \right|_{\overline{E_p}} < \frac{T_R}{\tau_L} r = \frac{T_R}{\tau_L} + \frac{E_p}{E_{sat,L}}. \qquad (2\text{-}15)$$

To benefit from the full modulation depth of the saturable absorber in CML lasers, the pulse energy must be high enough to bleach the absorber. To meet that condition, the pulse fluence on the SESAM should be approximately five times the absorber saturation fluence. With this approximation and the assumption of R_{ns}=1, as well as with relations (2-10) and (2-14), we obtain for the nonlinear reflectivity of the SESAM

$$R(E_p) \approx 1 - \Delta R \frac{F_{sat,A} A_{eff,A}}{E_p} \quad or \quad R(F_{P,A}) \approx 1 - \Delta R \frac{F_{sat,A}}{F_{P,A}}, \qquad (2\text{-}16)$$

where $F_{P,A}=E_p/A_{eff,A}$ is the pulse fluence incident upon the SESAM. At lower fluences the residual saturable absorption would contribute to the cavity loss and act against self-starting and efficient mode-locked operation.

If the laser operates with r >> 1 or at high power with P >> $P_{sat,L}$, we can neglect the first term on the right-hand side of relation (2-15), and the stability criterion of CML against QML becomes independent of the upper-state lifetime of the considered laser material. The saturation energy is then the only relevant parameter of the gain medium.

With the approximation listed above, stability condition (2-15) can be written in the following equivalent forms:

$$E_p^{\,2} > E_{sat,L} E_{sat,A} \Delta R \qquad (2\text{-}17)$$

$$F^2{}_{P,A} > F_{sat,L} F_{sat,A} \Delta R \frac{A_{eff,L}}{A_{eff,A}} \qquad (2\text{-}18)$$

$$P^2 > F_{sat,L} F_{sat,A} \Delta R A_{eff,L} A_{eff,A} \frac{1}{T_R{}^2} . \qquad (2\text{-}19)$$

With respect to the experimental verification of the theory, it is helpful to introduce the QML parameter $E_{sat,L}Es_{at,A}\Delta R$, because it contains all the parameters that determine the laser dynamics. We then define the critical intracavity pulse energy $E_{P,c}$ as the square root of the QML parameter:

$$\begin{aligned} E_{P,c} &\equiv (E_{sat,L} E_{sat,A} \Delta R)^{1/2} \\ &= (F_{sat,L} A_{eff,L} F_{sat,A} A_{eff,A} \Delta R)^{1/2} . \end{aligned} \qquad (2\text{-}20)$$

SESAM, as an intracavity saturable absorber first introduced by Keller et al. in 1992 [19], has successfully used to mode lock a wide range of lasers [19-23]. It can also be adapted to many wavelengths by using different combinations of semiconductor layers and material parameters [24]. The variable key parameters of SESAM, such as recovery time and saturation fluence, offer advantages over other saturable absorbers in other passively mode-locked lasers. In addition, the SESAM can be used as a cavity mirror, which makes the insertion loss much lower and much more compact cavity setup [5].

2.3. Passively Mode locking with NLM

Fig. 2.2 illustrates the basic idea of the nonlinear mirror. An intense light beam at frequency ω generates second harmonic SH in a nonlinear crystal NLC. The total second harmonic at 2ω and part of the fundamental F are reflected by a dichroic mirror M in the exact backward direction. In the second pass through the nonlinear crystal, partial reconversion of the second harmonic into fundamental takes place. The higher the intensity of the incident beam the

higher is the conversion into second harmonic and the higher is the amplification of the reflected fundamental due to the presence of the second harmonic wave. Hence one should expect that the resultant reflectivity increases with increase of the intensity of the incident beam. According the report by Stankov et al [7], we can rewrite the formula about the intensity dependent reflectivity as:

$$\begin{aligned} R_{NL} &= [\rho R_{2\omega} + (1-\rho) R_{\omega}] \\ &\times [1 - \tanh^2([\rho R_{2\omega} + (1-\rho) R_{\omega}]^{1/2} \\ &\times \arctan h\sqrt{\rho} - \arctan h\{(\rho R_{2\omega})^{1/2} \\ &\times [\rho R_{2\omega} + (1-\rho) R_{\omega}]^{1/2}\})]. \end{aligned} \qquad (2\text{-}21)$$

2.4. Cavity configuration

In order to make sure the laser cavity which was stable and allow the mode matching with the pump beam, we could use the ABCD law to determine the spot size at any position in the cavity [25]. Generally, we could calculate the ABCD matrix if we know all the optical components. As a result the Gaussian beam in the cavity can be described by

$$\frac{1}{\tilde{q}(z)} = \frac{1}{R(z)} - j\frac{\lambda}{\pi w^2(z)} \qquad (2\text{-}22)$$

where $\tilde{q}(z)$ is the complex beam parameter, R(z) is the radius of curvature of the wavefront, w(z) is the transverse dimension of the beam, and λ is wavelength. And

$$\tilde{q}_2(z) = \frac{A\tilde{q}_1(z) + B}{C\tilde{q}_1(z) + D}, \qquad (2\text{-}23)$$

where A, B, C, D are the matrix elements of the ABCD lens matrix, $\tilde{q}_1(z)$ is the complex beam parameter prior to the optical component, and $\tilde{q}_2(z)$ is the complex beam parameter after the optical component.

We assume that there is a complex beam parameter q(z), which describes the field on an arbitrary plane inside the cavity. We do not know its value at this stage, but we do know it does exist. We determine the value of q at the plane z by forcing the q to transform into itself after a round trip. This will give $\tilde{q}_1(z + round\ \ trip) = \tilde{q}_2(z) = \tilde{q}_1(z)$ and we use the fact that AD-BC=1. Applying the two conditions to (2-23), we have

$$\tilde{q}(z) = \frac{(A-D) \pm \sqrt{(D-A)^2 + A(AD-1)}}{2C} \qquad (2\text{-}24)$$

Thus (2-24) is the complex beam parameter at the beginning of the optical components, so we could substitute (2-23) into (2-22), we obtain

$$\omega(z) = \sqrt{\frac{\lambda}{\pi \,\mathrm{Im}[1/\tilde{q}(z)]}}. \qquad (2\text{-}25)$$

As the result of (2-25), we can determine the spot size at any position in cavity through the ABCD law.

2.5. The autocorrelator

There are two kinds of autocorrelator. One is interferometric autocorrelator and the other one is intensity autocorrelator. The front is also called the collinear autocorrelator. An overview of the approaches is presented in Fig. 2.3. The laser emits a continuous stream of mode-locked pulses. Each individual pulse is divided by a beam splitter into two equal intensity pulses. One of these pulses is delayed by τ seconds relative to the other. Two pulses being recombined again in a nonlinear optical crystal. The second harmonic (2ω) pulse generated by the crystal is incident on a power meter to detect the SHG power with the different delay time. Therefore, we could measure the

autocorrlator trace. We could describe these two pulses as

$$E_1(t) = \varepsilon(t)\exp(j\omega t) \qquad (2\text{-}26)$$

$$E_2(t) = \varepsilon(t-\tau)\exp(j\omega t)\exp(-j\omega t), \qquad (2\text{-}27)$$

where $\varepsilon(t)$ is the envelope function of the pulse. If the imaginary part of the $\varepsilon(t)$ changes with time, it will make a shift in frequency. This phenomenon is called chirping. While the two pulses achieve the condition of phase match in the SHG crystal, the electrical field of SHG is proportioned to $[E_1(t)+E_2(t)]^2$, and the intensity of SHG is proportioned to $|[E_1(t)+E_2(t)]^2|^2$. The power read by the power meter can be described :

$$P_{2\omega}(\tau) \propto \left\langle \left| E_1(t) + E_2(t) \right|^4 \right\rangle. \qquad (2\text{-}28)$$

We could substitute (2-26), (2-27) into (2-23) to get

$$\begin{aligned} P_{2\omega}(\tau) \propto\ & 2\left\langle \left|\varepsilon(t)\right|^4 \right\rangle + 4\left\langle \left|\varepsilon(t)\right|^4 \right\rangle + 4\left\langle \left|\varepsilon(t)\right|^2 \left|\varepsilon(t-\tau)\right|^2 \right\rangle \\ & + 4\,\mathrm{Re}\left\langle \varepsilon^2(t)\varepsilon(t)\varepsilon^*(t-\tau)\exp(j\omega\tau) \right\rangle \\ & + 4\,\mathrm{Re}\left\langle \varepsilon(t)\varepsilon(t-\tau)\varepsilon^*(t-\tau)^2\exp(j\omega\tau) \right\rangle \\ & + 2\,\mathrm{Re}\left\langle \varepsilon^2(t)\varepsilon^*(t-\tau)^2\exp(2j\omega\tau) \right\rangle. \end{aligned} \qquad (2\text{-}29)$$

At zero delay (τ=0) between the two pulses, we could get the highest SHG power $P_{2\omega}(\tau=0) = 16\left\langle \left|\varepsilon(t)\right|^4 \right\rangle$ and $P_{2\omega}(\tau >> \tau_d) = 2\left\langle \left|\varepsilon(t)\right|^4 \right\rangle$ when $\tau >> \tau_d$,.

The ratio of the background and the top of SHG power should reach 1:8

Autocorrelation measurements by second harmonic generation (SHG) are the most common means for evaluating the ultrashort pulse (Fig. 2.4). The laser emits a continuous stream of mode-locked pulses. Each individual pulse is divided by a beam splitter into two equal intensity pulses. One of these pulses is advanced by τ seconds relative to the other. Two pulses are recombined again in a nonlinear optical crystal. The second harmonic pulse generated by the crystal is incident on a slow detector whose output current is integrated over a time long compared to the optical pulse duration. Therefore, the output of slow detector is a function of delay time τ_d.

$$i_d \propto \left\langle I^2(t)\right\rangle + \left\langle I^2(t-\tau_d)\right\rangle + 4\left\langle I(t-\tau_d)\right\rangle, \qquad (2\text{-}30)$$

where the angle brackets signify time averaging and recognizing that $\left\langle I^2(t)\right\rangle = \left\langle I^2(t-\tau_d)\right\rangle$. The normalized detector output becomes:

$$i_d = 1 + 2G^{(2)}(t_d), \qquad (2\text{-}31)$$

where $G^{(2)}(t_d)$ is the second-order autocorrelation function of the intensity pulse and is defined by:

$$G^{(2)}(t_d) = \left\langle I(t)\right\rangle\left\langle I(t-\tau_d)\right\rangle \Big/ I^2(t). \qquad (2\text{-}32)$$

In the case of well-behaved ultrashort coherent light pulse of duration τ_d, we have $I_d(0) = 3$ and $i_d(\tau >> \tau_d) = 0$, since $G^{(2)}(0) = 1$ and $G^{(2)}(\tau >> \tau_d) = 0$. A plot of $i_d(\tau_d)$ versus τ will consist of a peak of zero delay and background of unit height. The central peak will have a width $\sim\tau_d$.

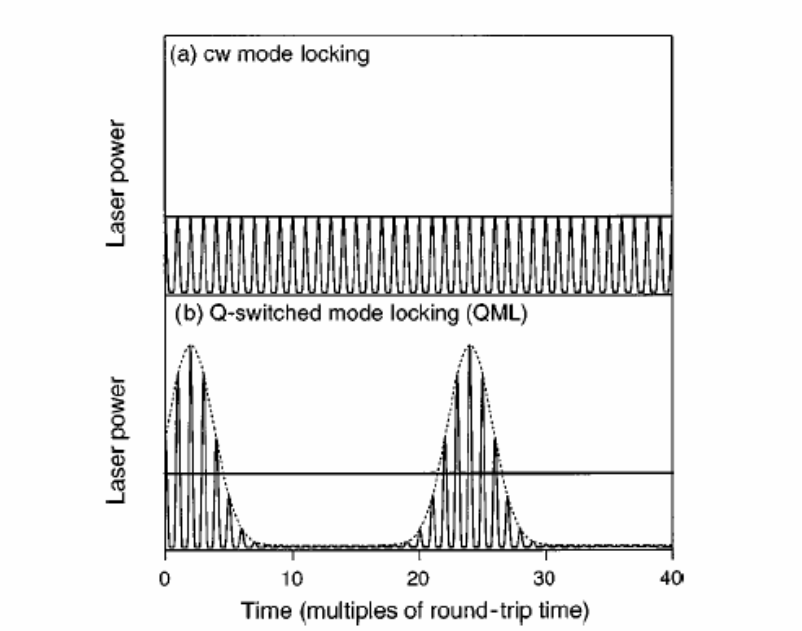

Fig. 2.1 Instantaneous and average laser power versus time.

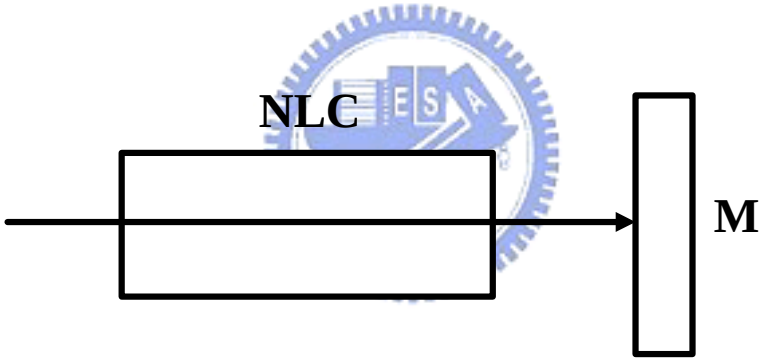

Fig. 2.2 Schematics of the nonlinear mirror mode-locking.

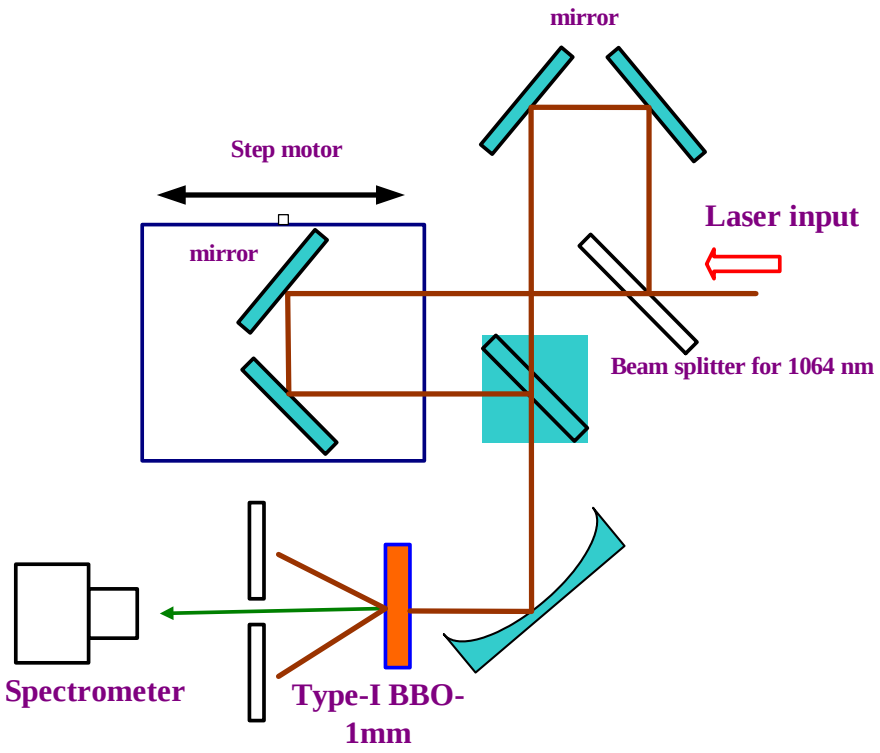

Fig. 2.3 Arrangement of basic principle second-order collinear autocorrelator.

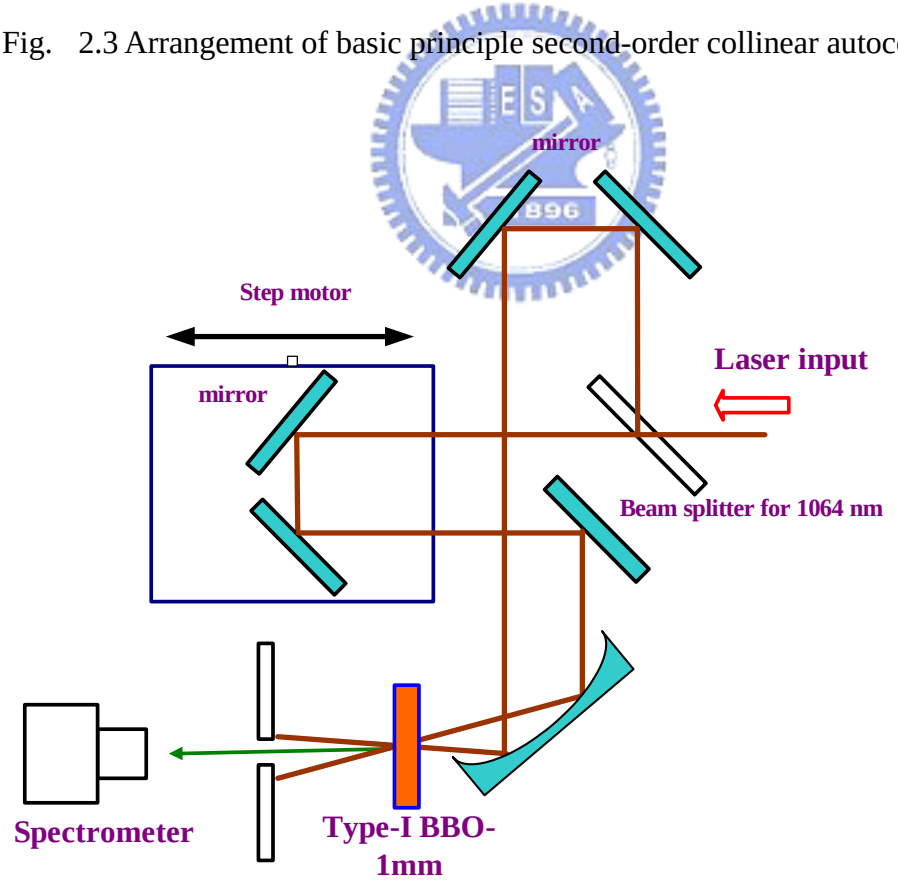

Fig. 2.4 Arrangement of a second-order noncollinear autocorrelator.

Chapter 3 Diode-Pumped Passively Mode-Locked Nd:GdVO4 Laser by a Semiconductor Saturable Absorber Mirror

3.1. Experiment setup

The schematic of the Z-shaped laser setup is shown in Fig. 3.1. A 4x4x8 mm^3 a-cut Nd:$GdVO_4$ crystal (with 0.5% Nd^{3+} concentration) is end-pumped by a fiber-coupled laser diode (FAP-81-16C-800-I, Coherent Inc.) at 808 nm. The pump beam coming out from the fiber is imaged on the crystal through the 1:1.8 optical imaging accessories (OIA's, Coherent Inc.). Therefore, the radius diameter of the pump beam in the gain medium (w_p) is around 225 μm that is slightly larger than the estimated radius of the cavity mode at the gain medium (w_g) around 210 μm by using the ABCD law [25] and considering the thermal lensing effect [26] on the Nd:$GdVO_4$. The laser crystal was wrapped with indium foil and mounted in a water-cooled copper block in which the water temperature was maintained at 15°C. One side of the Nd:$GdVO_4$ crystal is highly reflecting (HR) coated at 1064 nm and anti-reflecting (AR) coated at 808 nm pumping wavelength. The other side of the crystal with 2° wedge is AR coated at 1064 nm. In using SESAM, the laser cavity consists of two concave mirrors with M1 (the radius of curvature R= 500 mm) and M2 (R = 200 mm) as an output coupler (OC) mirror with the reflectivity of 90% at 1064 nm. The SESAM (from BATOP Optoelectronics) with the saturation fluence ~50 J/cm, saturation absorption 3.0%, and the relaxation time of 10 ps was cooled by TE-cooler at 20 °C and inserted in the cavity with the distance l_3 of 11 cm from the OC. The total length of the laser is 121cm with the distance l_1 of 30 cm from the laser crystal to M_1 and l_2=80 cm between two curved mirrors. A high speed InGaAs detector (Electro-Physics

Technology ET 3000) placed outside M1 was used to detect the small radiation of the cavity light (1064 nm) that was displayed on the oscilloscope (LeCroy LT372, Bandwidth 500MHz) and Rf spectrum analyzer (Hewlett Packard 8560E).

3.2. Results and discussion

The output power of the Nd:$GdVO_4$ laser were measured by the power meter (Scientech 365) in both CW mode locking (CML) and Q-switching mode locking (QML) state. The QML state (triangle) is initiated as the pumping power is beyond the threshold of the laser with the value of 1.4 W as shown in Fig. 3.2. The inset is the stable QML pulse train displayed on oscilloscope. Further increased the pumping power to about 4.7 W, we found stable CML state (circle). An average output power of 1.0 W from the CML Nd:$GdVO_4$ laser were obtained as the pump power was set up to 9 W. In Fig. 3.3, the regular CML pulse train with 8 ns spacing was displayed on the oscilloscope that corresponds to 124 MHz longitudinal frequency as shown in the RF spectrum. An 1 mm thick type-I BBO was used for the autocorrelation measurement. The measured autocorrelation intensity is shown in Fig. 3.4 with the duration of 15 ps FWHM, if a $sech^2$ pulse shape is assumed.

In the chapter 2, we have reviewed the theory developed by Kartner et. al. Here, we calculate the intracaviy pulse energy and compare with the critical intracavity pulse energy of the theoretical value as show in Fig. 3.5. The CML threshold (4.7 W) of our laser is close to the theoretical calculated value of 4.4 W. Finally, we did observe stable CML at P = 4.7W which is 3 times smaller than the previous reported result with the pump threshold of 13.7 W [5].

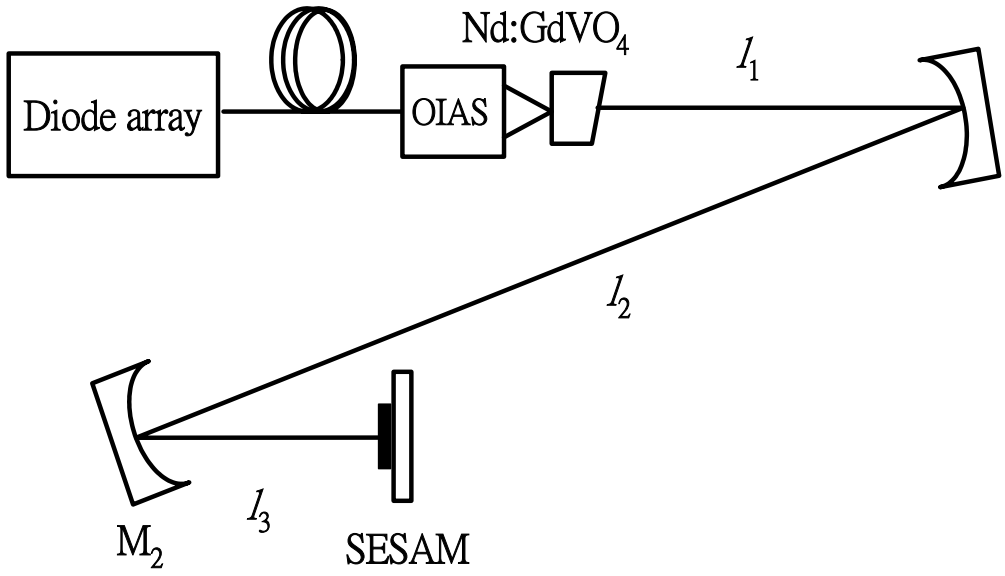

Fig. 3.1 Cavity configuration of the passively mode-locked Nd:$GdVO_4$ laser using SESAM.

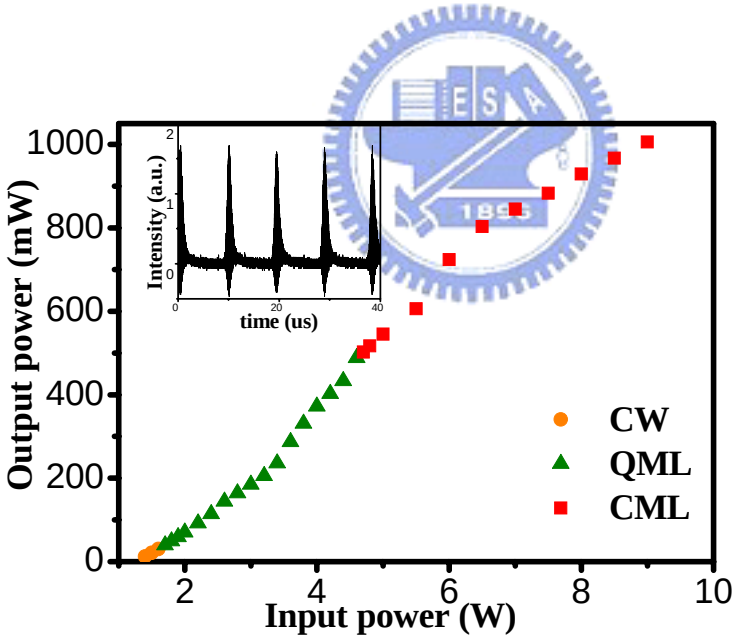

Fig. 3.2 Output power versus pump power for CW, QML and CML operations.

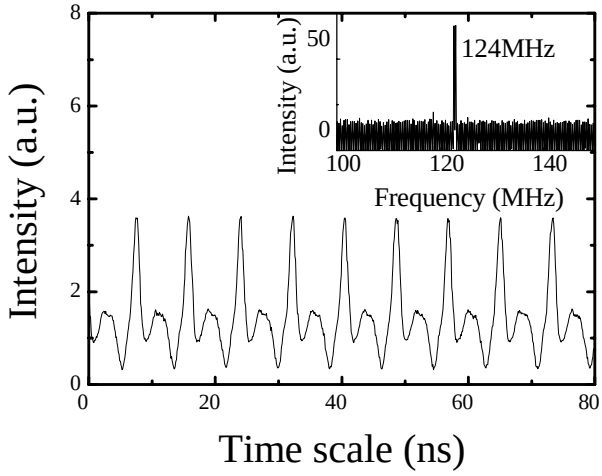

Fig. 3.3 Mode-locked pulse train and the power spectrum of the CML Nd:$GdVO_4$ laser.

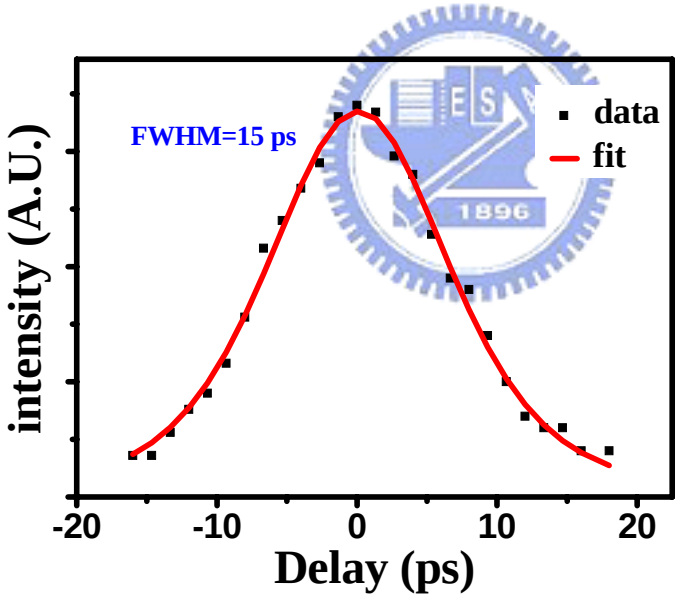

Fig. 3.4 Autocorrelation of the CML Nd:$GdVO_4$ laser using SESAM

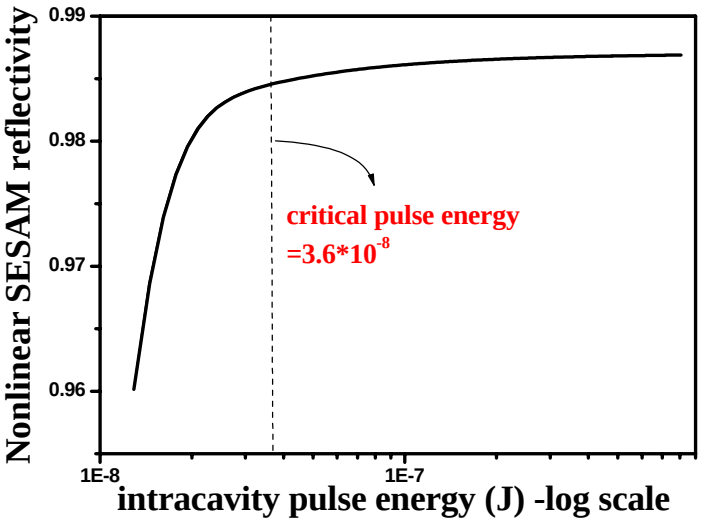

Fig. 3.5 Critical intra-cavity pulse energy for stable CML.

Chapter 4 Diode-pumped Nonlinear mirror mode-locked Nd:$GdVO_4$ laser

4.1. Experiment setup

In NLM, the setup is almost the same as in SESAM, except for an output coupler (OC) with the reflectivity of 80% at 1064 nm and high reflectivity at 532 nm, a 10 mm long type-II KTP crystal with antireflection coated at both faces for wavelength 1064 and 532 nm was placed very close to the dichroic OC mirror for the SH generation [Fig. 4.1].

4.2. Results and discussion

The output power of the Nd:$GdVO_4$ laser were measured by the power meter (Scientech 365) in both of the CW and the ML states. Fig. 4.2 shows the output power versus the pump power without and with the KTP insertion. The threshold pumping power of the CW lasing without KTP insertion is 1.2 W and the slope efficiency is 25%. The CW lasing threshold (~ 1.5 W) with KTP insertion is slightly higher than that without KTP insertion and its output power and slope efficiency are slightly lower. In comparing to the ratio of the output power (P_o) without and with KTP ($P_{o,KTP}$) at pump power of 10 W, we simply estimated the round-trip loss of the resonator to be L~ 0.2 according to the formula: $e^{-L}=P_{o,KTP}/P_o$. Using L=0.2 we calculated the linear loss, defined as $\gamma = L + Log[1+R_\omega] = 0.37$. The laser turns into stable QML at P_p=2.0 W before it reaches the CML state at P_p=2.3 W. An average output power is about 2.65 W from the CML Nd:$GdVO_4$ laser as the pump power raised to 10 W. Further

increasing the pump power will cause fluctuation of CML pulses or completely random pulsing due to thermal fluctuation of the KTP.

In Fig. 4.3, the typical pulse train of QML is displayed. The regular CML pulses show pulse spacing of 8.3 ns in Fig. 4.3 that corresponds to the repetition rate of 121 MHz. The measured autocorrelation is show in Fig. 4.4 with the duration of 38 ps (FWHM), if a $sech^2$ pulse shape is assumed. In addition, the corresponding spectrum measured by the spectrometer analyzer is show in the inset of Fig. 4.4 with the center wavelength of 1062.9 nm and FWHM of the bandwidth around 0.1 nm (AQ-6315A optical spectrum analyzer-resolution 0.01 nm).

The threshold power of 2.3 W for our stable CML is much lower than those of 9 W and 10 W for the NLM-ML Nd:YVO_4 mode-locked laser with 15 mm LBO [11] and 3 mm KTP [12], respectively. It is also much lower than 13.6 W for the Nd:$GdVO_4$ mode-locked laser with semiconductor saturable absorber mirror (SESAM) [5]. We therefore estimate the threshold for the CML against the QML as the intra-cavity peak power P_w exceeds the critical value (P_c) according to [17]:

$$P_\omega \geq P_c = (P_L P_A \Delta R_{\max})^{1/2} \quad , \qquad (4\text{-}1)$$

where P_L and P_A are the saturation power of the gain medium and the NLM "absorber", respectively, and ΔR_{max} is the maximum nonlinear modulation. Since the saturation intensity is related to the center frequency ω_o of the fundamental wave, the stimulated emission cross section σ_L=7.6 x10^{-19} (cm^2) and the fluorescence life time T_L=90 μs, according to $I_{sat} = \frac{\hbar\omega_o}{\sigma_L T_L}$ with $\hbar$ being the Planck constant, we estimated the saturation power of the gain medium P_L = $I_s(\pi W_g^2)$ to be 3.8 W. And the saturation power P_A of the NLM is defined as the

ratio of the linear loss Υ and the first order nonlinear loss modulation κ introduced by NLM absorber [11] which satisfies:

$$\kappa = -(dL_{nL}/dP_{\omega})_{P_{\omega}=0} = -(\rho/P_{\omega})R_{\omega}[R_{\omega}+1+2\cos(\Delta kl-\Delta\phi)], \qquad (4\text{-}2)$$

where L_{nL} is the round trip loss including the NLM, $\Delta\phi=\phi_{SH}-\phi_{FW}$ is the phase mismatch due to the dispersion of the air, and $\Delta k=k_{SH}-2k_{FW}$ is the wave vector mismatch between the FW and the SH in NLC. For low conversion efficiency, the coefficient of the conversion efficiency ρ from the FW to the SH can be presented as [27]

$$\rho(P_{\omega}) = \frac{P_{2\omega}}{P_{\omega}} = l^2(2\eta^3\omega^2 d^2{}_{eff})(\frac{P_{\omega}}{A})\frac{\sin^2(\Delta kl/2)}{(\Delta kl/2)^2}, \qquad (4\text{-}3)$$

where $P_{2\omega}$ is the intra-cavity peak power of the second harmonic wave, A is the area of fundamental beam at the KTP, l=1cm is the length of the KTP, η is the plane-wave impedance, and d_{eff}=3.18 (pm/v) is the effective second order nonlinear coefficient. In considering the strong modulation with the situation $\Delta k = 0$ and $\Delta\phi = \pi$, the maximum nonlinear loss is estimated with $\kappa_{max} = (\rho/P_{\omega})R_{\omega}(1-R_{\omega})$. Therefore, the saturation power $P_A = \Upsilon/\kappa_{max} = 6.9$ kW, and $\Delta R_{max} = 1-R_{\omega} = 20\%$, if the nonsaturable loss is nearly zero at high P_{ω}. Thus, the critical peak power (P_c) of CML for NLM is estimated around 72 W that can be reached as the pumping power is around 1.8 W as shown in Fig. 4.5. This value is slightly lower than our experimental result of 2.3 W for the stable CML that may be due to overestimating P_{ω} at lower pumping with the broader pulsewidth.

4.3. Picosecond pulse splitting and harmonic mode locking

As we knew, two-pulse generation of Kerr-lens mode-locked Ti:sapphire laser has been reported [28-30]. The most detailed experimental investigation on pulse splitting and multiple pulse operation had been performed in the works [31-32]. But there has no knowledge or phenomenon about pulse splitting in picosecond passive NLM mode-locked laser. In this thesis, we observed the pulse splitting by moving the nonlinear crystal in the cavity. When KTP is moved approach to the dichoric mirror, we observed the pulse splitting and harmonic mode locking from oscilloscope and rf spectrum analyzer. Besides, we also found that the average output power is increasing with moving the KTP. Shown in Fig. 4.6 are the pulse trains and corresponding rf spectra for the normal mode locking (NML), second mode locking (SHML), third mode locking (THML) and fourth mode locking (FHML), respectively. The NML is displayed on Fig. 4.6 (a) and (b) whose pulse train period is equal to cavity round trip time and the fundamental frequencies on rf spectrum are the multiple of longitudinal mode spacing. The time trace of the SHML in Fig. 4.6 (c) reveals that the numbers of pulses are twice of that in Fig. 4.6 (a). Furthermore, the spectral peaks at the first and third harmonics of longitudinal mode spacing are suppressed below the noise level in Fig. 4.6 (d) demonstrating the pulse trains with highly periodic. Similarly, THML and FHML are shown in Fig. 4.6 (e)~(h) with 1/3 and /14 times cavity round trip period pulse spacing in time traces.

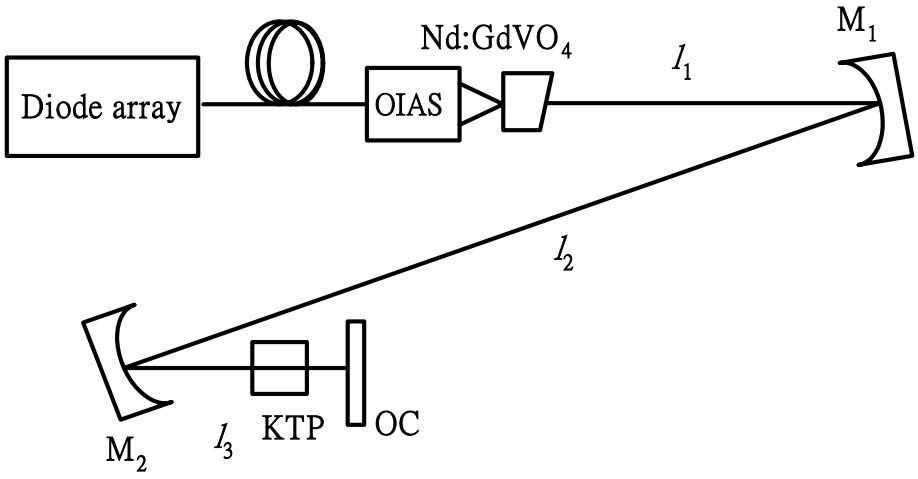

Fig. 4.1 Cavity configuration of the passively mode-locked Nd:$GdVO_4$ laser using NLM.

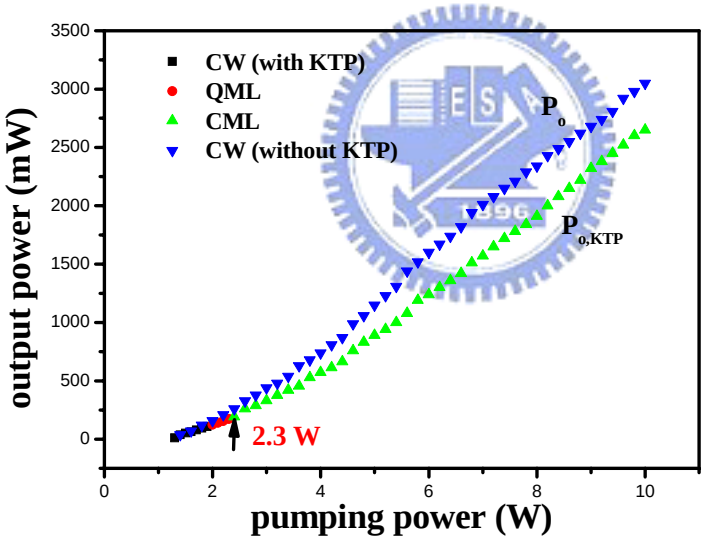

Fig. 4.2 Output power versus pump power for CW, QML CML operations using NLM.

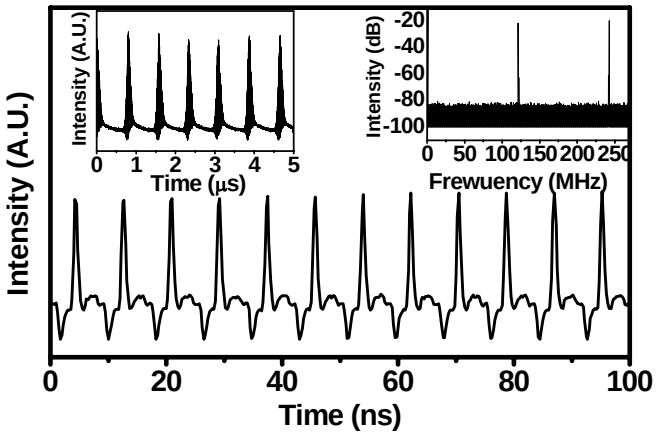

Fig. 4.3 CML pulse trains with the repetition rate of 121 MHz and it's rf spectrum and QML pulse trains.

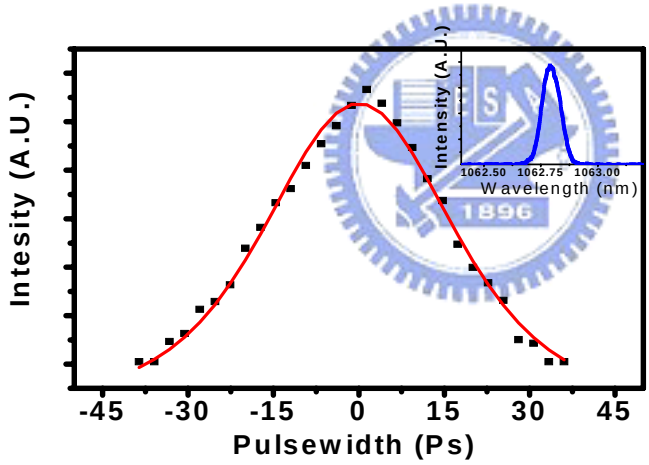

Fig. 4.4 Autocorrelation curve of the pulse duration and it's corresponding optical spectrum.

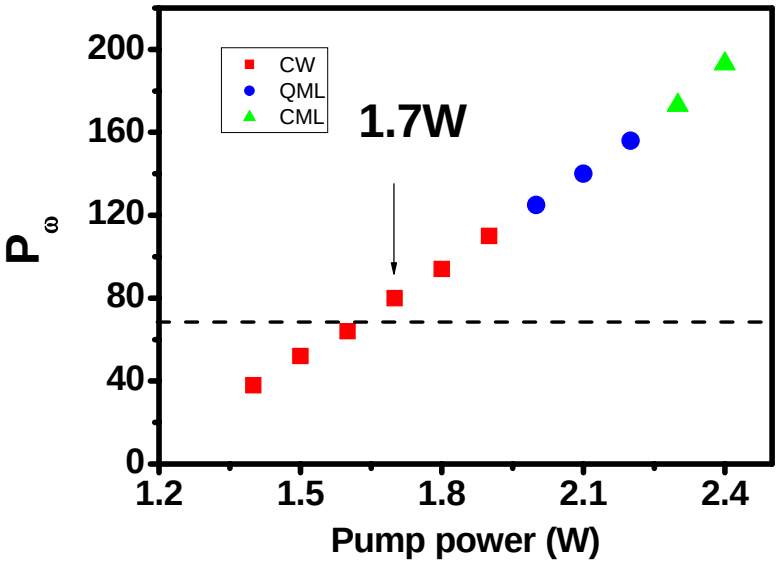

Fig. 4.5 Critical intra-cavity power for stable CML

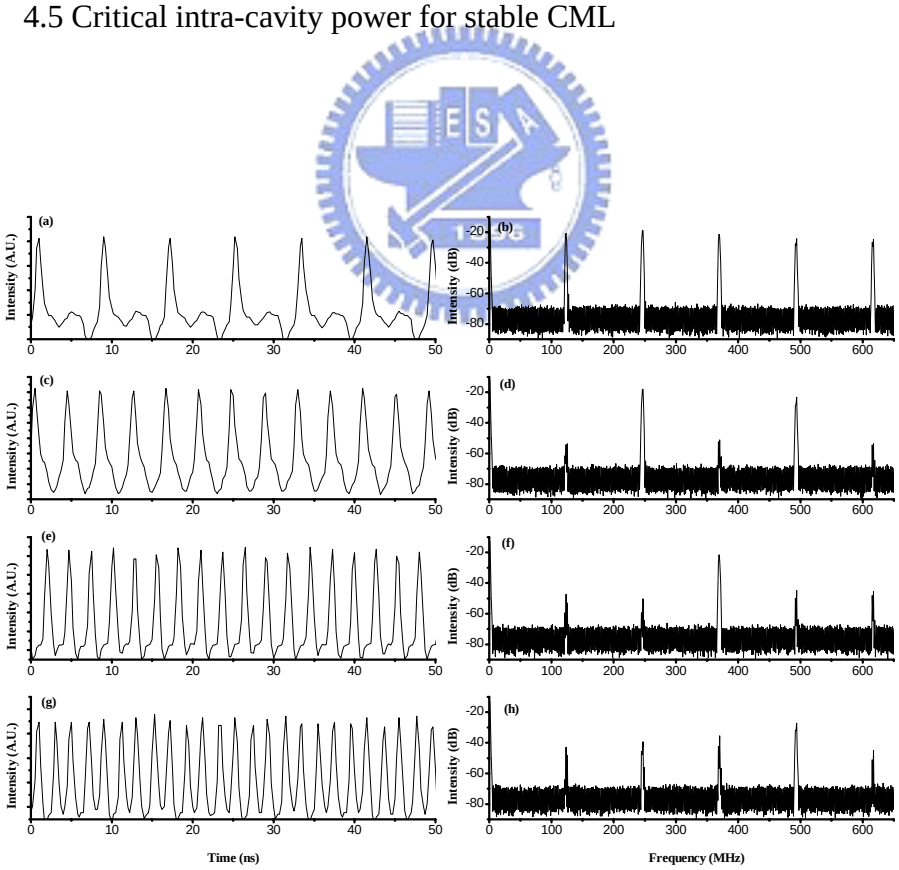

Fig. 4.6 Pulse trains for the NLM, SHML, THML, and FHML and their corresponding rf spectra.

Chapter 5 Conclusion and future works

5.1. Conclusion

We demonstrated two low threshold passive mode-locked Nd:$GdVO_4$ lasers. One is using SESAM and the other one is using nonlinear mirror with 1 cm KTP crystal. As increasing the pumping power, the laser output changes from CW, QML to CML in both lasers and two absorbers. Using SESAM, the CML threshold and pulse duration are 4.7 W and 15 ps. According to the Ref.15, we calculated the theoretical value of CML threshold to be 4.4 W, which is very close to our experiment value of 4.7 W and much lower than the result of the other group [5]. In using NLM, the CML threshold and pulse duration are 2.3 W and 38 ps. The CML threshold of NLM is also close to the theoretical value of 1.7 W in considering the reflection change as a function of pumping power.

Besides, we have for the first time observed the pulse splitting and harmonic mode locking by varying the distance between KTP and dichroic mirror in the NLM picosecod laser.

5.2. Future works

There are several works which are valuable to be studied in the future. First of all, we will investigate the mechanisms of harmonic ML and pulse splitting in NLM. Second, we will convert the stable picosecond ML laser to generate the third and fourth harmonics as the excitation source for time-resolved PL measurement of the ZnO nanostructures. Finally, we plan to investigate the supercontinnum generation by launching the picosecond ML laser pulses into the photonic crystal fibers.

References

1. H. D. Jiang, H. J. Zhang, J. Y. Wang, H. R. Xia, X. B. Hu, B. Teng, and C. Q. Zhang, "Optical and laser properties of Nd:$GdVO_4$ crystal," Opt. Commun. 198. 447 (2001).
2. J. kong, D. Y. Tang, S. P. Ng, B. Zhao, L. J. Qin, and X. L. Meng, "Diode-pumped passively mode-locked Nd:$GdVO_4$ laser with a GaAs saturable absorber mirror," Appl. Phys. B-Lasers And Optics, 79. 203 (2004).
3. S. Zhang, E Wu, H. Pan, and H. Zeng, "Q-switched mode-locking with Cr^{4+} : YAG in a diode pumped Nd : $GdVO_4$ laser," Appl. Phys. B-Lasers and Optics, 78, 335 (2004).
4. L. Krainer, D. Nodop, G. J. Spühler, S. Lecomte, M. Golling, and R. Paschotta, D. Ebling, T. Ohgoh and T. Hayakawa, K. J. Weingarten, and U. Keller, "Compact 10-GHz Nd:$GdVO_4$ laser with 0.5-W average output power and low timing jitter," Opt. Lett. 29, 2629 (2004).
5. S. Zhang, E. Wu, H. Pan and H. Zeng, "Passive mode locking in a diode-pumped Nd:$GdVO_4$ laser with a semiconductor saturable absorber mirror," IEEE J. Quantum. Electron. 40, 505 (2004).
6. Ja-Hon Lin, Ming-Dar Wei, Wen-Feng Hsieh, and Hsiao-Hua Wu, "Cavity configurations for soft-aperture Kerr-lens mode locking and multiple-period bifurcations in Ti:sapphire lasers ," J. opt. Soc. Am. B 18, 1069 (2001).
7. K. A. Stankov, "A Mirror with an Intensity-Dependent Reflection Coefficient," Appl. Phys. B, 45,191 (1988).
8. K. A. Stankov, "25 ps pulses from a Nd:YAG laser mode locked by a

frequency doubling β-BaB_2O_4 crystal," Appl. Phy. Lett, 58, 2203 (1991).

9. G. Cerullo, M. B. Danailov, S. De Silvestri, P. Laporta, V. Magni, D. Segala and S. Taccheo, "High power diode-pumped Nd:YAG regenerative amplifier for picosecond pulses," Appl. Phys. Lett, 65, 2392 (1994).
10. P. K. Datta, S. Mukhopadhyay, S. K. Das, L. Tartara, A. Agnesi, and V. Degiorgio, " Enhancement of stability and efficiency of a nonlinear mirror mode-locked Nd:YVO_4 oscillator by an active Q-switch," Opt. Express. 12, 4041 (2004).
11. P. K. Datta, S. Mukhopadhyay, and A. Agnesi, " Stability regime study of a nonlinear mirror mode-locked laser," Opt. Commun. 230, 411 (2004).
12. Y. F. Chen, S. W. Tsai, and S. C.Wang, " High-power diode-pumped nonlinear mirror mode-locked Nd:YVO_4 laser with periodically-poled KTP," Appl. Phys. B-Laser and Optics, 72, 395 (2001).
13. L. Fornasiero1, S.Kück, T. Jensen, G. Huber, and B. H. T. Chai, " Excited state absorption and stimulated emission of Nd^{3+} in crystals. Part 2: YVO_4 , $GdVO_4$, and Sr_5 $(PO_4)_3$ F," Appl. Phys. B-Laser and optics, 67, 549 (1998).
14. Ultrashort laser pulse and applications by W. Kaiser (Springer-Verlag,Berlin,1998).
15. Yariv, A., "Internal modulation in multimode laser oscillators", J. Appl. Phys.36, 388 (1965).
16. DiDomenico, M., Jr., "Small signal analysis of inter nal modulation of Lasers", J. Appl. Phys.36, 3870 (1964).
17. C. Hönninger, R. Paschotta, F. Morier-Genoud, M. Moser, and U.

Keller, " Q -switching stability limits of continuous-wave passive mode locking ," J. Opt. Soc. Am. B 16, 46 (1999).

18. H. A. Haus, "Parameter ranges for cw passave modelocking," IEEE. J. Quantum. Electron. 12, 169 (1976).
19. U. Keller, D. A. B. Miller, G. D. Boyd, T. H. Chiu, J. F. Fergusion, and M. T. Asom, "Solid-state low-loss intracavity saturable absorber for Nd:YLF lasers: an antiresonant semiconductor Fabry-Perot saturable absorber," Opt. Lett. 17, 505 (1992).
20. K. J. Weingarten, U. Keller, T. H. Chin, and J. F. Fergusion, " Passively mode-locked diode-pumped solid-state-lasers that use an antiresonant Fabry - Perot saturable absorber," Opt. Lett. 18, 640 (1993).
21. R. Fluck, G. Zhang, U. Keller, K. J. Weingarten, and M. Moser, " Diode-pumped passively mode-locked 1.3- mu m Nd:YVO_4 and Nd:YLF lasers by use of semiconductor saturable absorbers," Opt. Lett. 21, 1378 (1996).
22. B. Braun, C. Hönninger, G. Zhang, U. Keller, F. Heine, T. Kellner, and G. Huber, " Efficient intracavity frequency doubling of a passively mode-locked diode-pumped neodymium lanthanum scandium borate laser," Opt. Lett. 21, 1567 (1996).
23. U. Keller, T. H. Chiu, and J. F. Fergusion, " Self-starting femtosecond mode-locked Nd:glass laser that uses intracavity saturable absorbers," Opt. Lett. 18, 1077 (1993).
24. M. Haiml, R. Grange, and U. Keller, " Optical characterization of semiconductor saturable absorbers," Appl. Phys. B-Laser and Optics, 79, 331 (2004).

25. Laser Electronics edited by Joseph T. Verdeyen, 1981, chapter 5.
26. H. Zhang, J. Liu, J. Wang, C. Wang, L. Zhu, Z. Shao, X. Meng, X. Hu, M. Jiang, and Y. T. Chow, "Characterization of the laser crystal Nd:$GdVO_4$", J. Opt. Soc. Am. B 19, 18 (2002).
27. W. Koechner, *Soild-state laser engineering*, E. D. A. L. Schawlow, A. E. Siegman, T. Tamir, fifth ed., (Springer, Berlin, Heidelberg, 1999).
28. J.-C. Diels, and W. Rudolph, *Ultrashort Laser Pulse Phenomena*, Academic Press, San Diego, 1996.
29. D. R. Dykaar, S. B. Darack, and W. H. Knox, "Cross-locking dynamics in a two-color mode-locked Ti:sapphire laser," Opt. Lett. 19, 1058 (1994).
30. A. Leitenstorfer, C. Furst, and A. Laubereau, "Widely tunable two-color mode-locked Ti:sapphire laser with pulse jitter of less than 2 fs," Opt. Lett. 20, 916 (1995).
31. M. Lai, J. Nicholson, and W. Rudolph, "Multiple pulse operation of a femtosecond Ti:sapphire laser," Opt. Commun. 142, 45 (1997).
32. C. Wang, W. Zhang, K. F. Lee, and K. M. Yoo, "Pulse splitting in a self-mode-locked Ti:sapphire laser," Opt. Commun. 137, 89 (1997).